

A Study in Crystal Engineering: Structure, Crystal Growth, and Physical Properties of a Polar Perhydrotriphenylene Inclusion Compound

Olaf König,[†] Hans-Beat Bürgi,^{*,‡} Thomas Armbruster,[‡] Jürg Hulliger,^{*,†} and Thomas Weber[§]

Contribution from the Department of Chemistry and Biochemistry, and the Laboratory of Chemical and Mineralogical Crystallography, University of Berne, Freiestrasse 3, CH-3012 Berne, Switzerland, and Institute of Crystallography and Applied Mineralogy, Ludwig-Maximilians-University of Munich, Theresienstrasse 41, D-80333 Munich, Germany

Received June 12, 1997[⊗]

Abstract: Racemic perhydrotriphenylene (PHTP) forms a polar inclusion compound with 1-(4-nitrophenyl)piperazine (NPP) as a guest molecule. Homochiral stacks of PHTP molecules surround polar chains of hydrogen-bonded NPP molecules in a *channel*-type, honeycomb architecture. The NPP chains are arranged in an all-parallel (rather than an antiparallel) fashion. Crystals of [PHTP]₅[NPP] show second harmonic generation for incident light of wavelength 1064 nm, an electro-optical and a pyroelectric effect. The X-ray diffraction pattern exhibits Bragg-like reflections, interspersed with planes of diffuse scattering and weak satellite reflections superimposed on these planes, features which are indicative of extensive disorder. In spite of this, an orthorhombic average structure model could be deduced from the Bragg-like reflections (space group *Cmc*2₁, *a* = 15.023(2), *b* = 23.198(2), and *c* = 4.730(1) Å (*T* = 100 K), *wR*₂ = 0.088, goodness of fit 1.38). A qualitative interpretation of diffuse and satellite scattering is given. Crystals of [PHTP]₅[NPP] are approximately hexagonal prisms. If the tailor-made additive 1-(*p*-tolyl)piperazine (TP) is present during crystallization, the habit changes to approximately hexagonal plates and TP is incorporated in small amounts. Crystals of the composition [PHTP]₅[NPP]_{0.93}[TP]_{0.07} lose the ability of second harmonic generation. The observation of polar properties for a crystal structure whose polar building blocks, the -NO₂···HN- hydrogen-bonded NPP chains, are 14–15 Å apart and separated by PHTP hydrocarbon molecules is surprising, but can be explained in terms of a Markov chain model of crystal growth. The same simple model accounts for the loss of polarity in the presence of the tailor-made additive TP. The knowledge gained during the present analysis provides a rational tool for the engineering of polar properties of PHTP and similar channel-type inclusion compounds.

Introduction

A general method for producing materials with nonlinear optical (NLO) and electro-optical (EO) properties¹ is the incorporation of polar molecules with high hyperpolarizability into crystalline inclusion lattices. The methods of molecular and supramolecular engineering² are useful in the design and geometrical optimization of such structures which need to be polar if they are to show the desired pyroelectrical, EO, and second-order NLO effects. Host compounds such as thiourea, tris-*o*-thymotide, deoxycholic acids, or perhydrotriphenylene (PHTP), form channel-type inclusion compounds with a great variety of dipolar guest molecules and with a high incidence of polar structures.³ PHTP is an especially interesting host because it includes a large number of today's most efficient NLO molecules and forms polar inclusion lattices with more than 90% of the molecules investigated in cocrystallization experi-

ments.⁴ By comparison, the same molecules crystallized as pure compounds form polar structures with a probability of only about 30%.⁴

The pioneering work of M. Farina and co-workers on the solid state and structural chemistry of PHTP inclusion compounds has been reviewed recently.⁵ Farina's group has shown in the late 1960s that PHTP molecules form stacks which aggregate into hexagonally shaped channels (Figure 1). These channels contain the guest molecules. Due to heavy disorder, Farina et al. have not determined the exact positions of the included molecules.⁶ Thus, there is a need for information on the detailed arrangement of the guest molecules.

Here we describe, for the first time, the structural details of both the host and guest arrangements in a *polar PHTP inclusion compound* with 1-(4-nitrophenyl)piperazine (NPP) as the guest. A single-crystal analysis was possible in spite of the presence of severe, two-dimensional diffuse scattering located between a sharp, Bragg-like diffraction pattern.⁷ X-ray crystallography and measurements of physical properties indicate a polar solid state structure of [PHTP]₅[NPP] at both the microscopic and

[†] Department of Chemistry and Biochemistry, University of Berne.

[‡] Laboratory of Chemical and Mineralogical Crystallography, University of Berne.

[§] Ludwig-Maximilians-University of Munich.

[⊗] Abstract published in *Advance ACS Abstracts*, October 1, 1997.

(1) Bosshard, C.; Sutter, K.; Prêtre, P.; Hulliger, J.; Flörshäuser, M.; Kaatz, P.; Günter P. *Organic Nonlinear Optical Materials*. In *Series Advances in Nonlinear Optics*; Garito, A. F. J., Kajzar, F., Eds.; Gordon and Breach: New York, 1995; Vol. 1.

(2) Lehn, J. M. *Supramolecular Chemistry: Concepts and Perspectives*; VCH, Weinheim, 1995.

(3) Eaton, D. F.; Anderson, A. G.; Tam, W.; Wang, Y. *J. Am. Chem. Soc.* **1987**, *109*, 1886–1888. For a review, see: Ramamurthy, V.; Eaton, D. F. *Chem. Mater.* **1994**, *6*, 1128–1136.

(4) Hoss, R.; König, O.; Kramer-Hoss, V.; Berger, U.; Rogin, P.; Hulliger, J. *Angew. Chem., Ed. Int. Engl.* **1996**, *35*, 1664–1666. König, O.; Hulliger, J. *Nonlinear Optics (Mol. Cryst. Liq. Cryst. Sci. Technol. Sect. B)* **1996**, *17*, 127–139.

(5) Farina, M.; di Silvestro, G.; Sozzani, P. In *Comprehensive Supramolecular Chemistry, Vol. 6, Solid-State Supramolecular Chemistry: Crystal Engineering*; MacNicol, D. D., Toda, F., Bishop, R., Eds.; Pergamon Press: New York, 1997.

(6) Allegra, G.; Farina, M.; Immirzi, A.; Colombo, A.; Rossi, U.; Broggi, R.; Natta, G. *J. Chem. Soc. B* **1967**, 1020–1028.

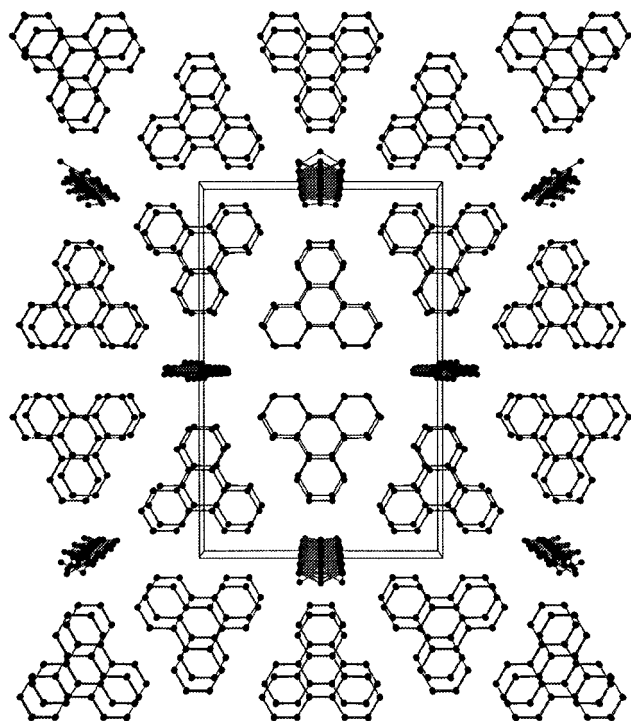


Figure 1. Projection of the molecular packing of the inclusion compound [(±)-PHTP]₅[NPP] along the channel axis *c*.

macroscopic lengths scales. Related observations on crystallization phenomena are also presented.

Issues to be discussed include the adaptability of the host lattice to the shape of the guest molecules, guest–guest interaction along the channels, and guest–host–guest correlation between adjacent channels. These aspects are relevant for the development of channel-type supramolecular materials whose EO and other polar tensorial properties are both electronically and geometrically optimized.

The results presented here raise the rather fundamental question about the supramolecular mechanism responsible for the macroscopically polar arrangement of guest molecules. While it is easy to see that intermolecular interactions of NLO guest molecules favor formation of polar chains along individual channels, it is not so obvious why different channels separated by ~ 15 Å show the same direction of polarity. In this work, we present a general mechanism, coined in terms of Markov's theory of stochastic processes, which explains the high yield of structures with macroscopic polar properties, and the suppression of such properties by a tailor-made additive.

Experimental Procedures

Crystallization of the Inclusion Compounds. Pure racemic PHTP was synthesized as described in ref 8. Enantiomerically pure (–)-PHTP was obtained from Prof. P. Sozzani, University of Milan, and from our own separation experiments using affinity chromatography with a modified β -cyclodextrin as the stationary phase. Details of the enantiomeric separation will be published elsewhere. NPP was purchased from Aldrich and was purified by recrystallization from 2-butanone before use.

The inclusion compound [(±)-PHTP]₅[NPP] was crystallized from a 2-butanone solution 0.04 M in PHTP and 0.053 M in NPP by a temperature difference technique ($\Delta T = 2$ K), described elsewhere.⁸

(7) For related studies on urea–alkane inclusion compounds which show even more complicated diffuse scattering, see, for example: Weber, Th.; Boysen, H.; Honal, M.; Frey, F.; Nader, R. B. *Z. Krist.* **1996**, *211*, 238; Fukao, K. *J. Chem. Phys.* **1994**, *101*, 7882. For reviews on diffuse scattering, see: Welberry, T. R.; Butler, B. D. *Chem. Rev.* **1995**, *95*, 2369. Frey, F. *Acta Crystallogr.* **1995**, *B51*, 592; *Z. Krist.* **1997**, *212*, 257.

Crystals of [PHTP]₅[NPP] form as yellowish needles up to several millimeters in length. They show a dichroism, appearing dark yellow when illuminated with light polarized parallel to the needle axis.

Alternative methods for obtaining crystals of [(±)-PHTP]₅[NPP] include controlled isothermal evaporation, solid state reaction, sublimation, and crystallization from the melt. For isothermal evaporation, a solution of 2-butanone or paraldehyde containing (±)-PHTP and NPP in a weight ratio of 4:1 is slowly supersaturated in a glass cup with a silanated surface or in a Teflon vessel, which is placed in a temperature controlled chamber ($T = 300$ K). For solid state synthesis, crystalline (±)-PHTP and NPP are ground with the help of a mortar and pestle followed by annealing at 380 K over a period of 24 h.⁴ Crystallization of [(±)-PHTP]₅[NPP] from the gas phase is performed by evaporating the starting materials from Knudsen cells⁸ and condensing on a cold finger at 260 K or by physical vapor transport in a sealed ampule with a temperature gradient of $\Delta T < 1$ K at $T = 380$ K. [(±)-PHTP]₅[NPP] also crystallizes from a homogenous [PHTP]₅[NPP] melt at $T = 429$ K (the melting points of the pure compounds are 403 K for (±)-PHTP and 410 K for NPP).

Contrary to racemic (±)-PHTP, (–)-PHTP showed a preference to coinclude 2-butanone *within* the channels. It was therefore necessary to employ paraldehyde as the solvent, which by its van der Waals diameter of ~ 8 Å is far too large to permit coinclusion.

Cocrystals of (–)-PHTP and NPP were grown by controlled isothermal evaporation of a paraldehyde solution and by sublimation in a sealed ampule. In both cases, the crystals obtained were unsuitable for a full structure analysis, since they showed several orientations of the crystallographic *a* and *b* axes with no obvious relationship between orientations. Their quality was, however, sufficient for an X-ray rotating crystal photograph which confirmed the formation of the inclusion lattice and allowed the measurement of the stacking period of (–)-PHTP host molecules.

Solid solutions of [(±)-PHTP]₅[(NPP)_{1-x}(TP)_x] (TP, 1-(*p*-tolyl)-piperazine) were prepared by the temperature difference technique ($\Delta T = 2$ K).⁸ The concentration of TP in the initial solution saturated in NPP (298 K) was increased in steps of 5 mg per mL of paraldehyde. Crystals were collected after each step of adding TP. Due to the high solubility of TP, no solid excess of TP was present during the crystallization experiments.

The composition of the inclusion compounds was analyzed by ¹H NMR spectroscopy and gas chromatography; no inclusion of solvent molecules has been observed either in pure [PHTP]₅[NPP] or in the solid solutions with TP.

Second Harmonic Generation (SHG), Pyroelectric, and Electro-optic (EO), Measurements. Qualitative SHG measurements were performed with a Q-switched Nd:YAG laser operating at 1064 nm. Fine-grain powder samples (average particle size ≈ 50 μ m) or some small single crystals of racemic [PHTP]₅[NPP], as well as of (–)-[PHTP]₅[NPP], showed intense emission of green light (to the naked eye) indicative of an SHG effect. The effect cannot be due to pure (±)-PHTP and NNPP, which crystallize in centrosymmetric space groups and show no SHG activity. SHG experiments were done for [(±)-PHTP]₅[NPP] crystals obtained from the temperature difference technique, isothermal evaporation, sublimation, and melt and from the solid state reaction. In *all* cases, the samples exhibited a clear SHG effect; thus, there is no evidence to suggest that the method of crystal preparation or the surface of the crystallization vessel has any influence on the SHG effectivity of the [(±)-PHTP]₅[NPP] crystals. SHG experiments on a number of broken pieces of a single crystal with composition [PHTP]₅[(NPP)_{0.93}(TP)_{0.07}] were also performed, but no SHG effects could be detected visually.

The polarity of the [PHTP]₅[NPP] crystals has also been confirmed by measurements of the pyroelectric effect.⁹ Crystals of [PHTP]₅[NPP] were placed between the plates of a capacitor with their *c* axis perpendicular to these plates. Needles which are ~ 2 –3 mm long were scanned with a laser diode beam of 20 μ m in diameter. This induces a local temperature change ΔT accompanied by a change of polarization *P*. The concomitant change in the surface charge density of the crystal was monitored by measuring the discharge current of the capacitor under

(8) Hulliger, J.; König, O.; Hoss, R. *Adv. Mater.* **1995**, *7*, 719–721. Hulliger, J. *Angew. Chem., Int. Ed. Engl.* **1994**, *33*, 143–146.

(9) Quintel, A.; Wübbenhorst, M.; Hulliger, J. *J. Phys. Chem.* Submitted.

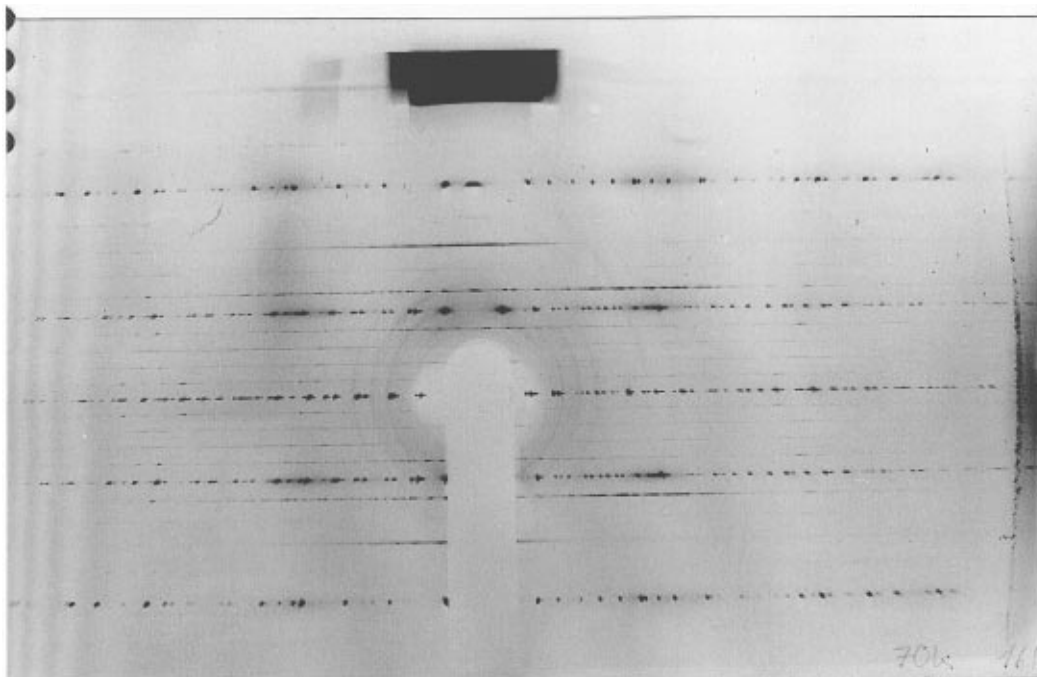


Figure 2. Oscillation photograph of a crystal of [(±)-PHTP]₅[NPP] around the c^* axis ($\pm 30^\circ$; Cu $K\alpha_1$ radiation; exposure time 16 h; $T = 100$ K).

zero-field conditions. The pyroelectric displacement current changes direction in the middle of selected crystals indicative of inversion of polarity. This observation suggests formation of polar domains which are several hundred micrometers to several millimeters in length.

The presence of an EO effect was demonstrated by embedding a wedge-shaped single crystal of racemic [(±)-PHTP]₅[NPP] in a transparent epoxy resin, placing the sample under a polarizing microscope, and illuminating perpendicular to one of the wedge planes with a polarized HeNe laser beam. Under the influence of a static electric field of $\sim \pm 3$ kV/cm oriented perpendicular to the laser beam and approximately parallel to the channel axes, the interference fringes produced by the laser beam showed a small, but homogeneous, displacement ($\pm \delta$) depending on the polarity of the electric field. This measurement gives an average result over the thickness of the sample with low resolution along the channel axis ($\sim 100 \mu\text{m}$). It nevertheless demonstrates that the two crystals investigated, each of them a few millimeters long, show an EO effect. In the EO experiments described above we happened to deal with crystals showing no inversion of polarity. Such crystals are obtained if the area around one end of a needle-shaped seed provides no free space for crystal growth.

X-ray Diffraction Analysis. Single-crystal oscillation and precession photographs of the inclusion compound [(±)-PHTP]₅[NPP] taken at room temperature show a repeating pattern of equally spaced planes in reciprocal space with diffuse and sharp scattering features (Figure 2). Every fifth plane shows only Bragg-like, sharp diffraction spots, whereas the scattering associated with the four planes in between is essentially continuous within the planes and sharp perpendicular to them. A set of relatively distinct but weak reflections is superimposed on the diffuse planes. The photographs indicate orthorhombic *mmm* Laue symmetry for the full diffraction pattern. The diffraction features have been indexed on the basis of an orthorhombic unit cell with $a = 15.023 \text{ \AA}$, $b = 23.198 \text{ \AA}$, $c' = 23.65 \text{ \AA}$ ($T = 100$ K), corresponding to integer l' -indices for the diffuse planes. The indices of the Bragg reflections are $h,k,5i$ with h,k,i all integer. The pattern of weak reflections differs on the diffuse planes $l' = 5i \pm 1$ and $l' = 5i \pm 2$. The position of the weak reflections in reciprocal space can be described in terms of a^* , b^* , and c'^* as $h \pm 0.62(1), k, 5i \pm 1$ ($h + k$ even) and $h, k, 5i \pm 2$ ($h + k$ odd) with h, k, i all integers.

Oscillation photographs taken at 55, 70, 100, 120, 140, 160, and 200 K show essentially the same features as those taken at room temperature (Figure 2). An oscillation picture of [(-)-PHTP]₅[NPP] taken at room temperature gives $c' = 23.83(2) \text{ \AA}$, the same as that found for [(±)-PHTP]₅[NPP]. The diffraction pattern of the solid solution [PHTP]₅[(NPP)_{0.93}(TP)_{0.07}] has the same general appearance as that of the pure [(±)-PHTP]₅[NPP] system.

The rather complicated diffraction pattern is interpreted in three steps: First the diffuse and Bragg-like scattering is discussed qualitatively; next, the Bragg-like diffraction is analyzed quantitatively; and finally, some remarks about the satellite reflections are added.

The sharpness of all diffraction features in the c^* -direction indicates translational order along c with a period of 23.65 \AA ($T = 100$ K). The diffuse nature of the scattering in the a^*, b^* plane for $l' \neq 5i$ is incompatible with perfect translational order in the a and b directions. However, the Bragg-like, sharp reflections with integer indices $h, k, 5i$ indicate a residual long-range order also in the a, b plane which is probabilistic in nature. Specifically, the presence of these reflections requires that the fractional coordinates of an atom j anywhere in the crystal can be written as $x_j + m, y_j + n, z_j' + p + q(m, n)/5$ with m, n, p , and q integers and $0 \leq q(m, n) \leq 4$. The values of q are associated with a probability $P[q(m, n)]$, as a yet unknown function of the translational vectors ma and nb .

Alternatively, the Bragg-like reflections can be interpreted as arising from an averaged crystal structure obtained by slicing the unit cell perpendicular to c' into five slabs of thickness $c'/5$ and superimposing them all on top of each other. In either case, the structure factor expression $F(h, k, l')$ for $l' = 5i$ becomes

$$F(h, k, l') = \sum_j f_j \exp 2\pi i [hx_j + ky_j + 5i(z_j' + q(m, n)/5)]$$

Since $5iq/5$ is always integer, this leads to

$$F(h, k, l') = \sum_j f_j \exp 2\pi i (hx_j + ky_j + 5iz_j')$$

With the transformations $c = c'/5$, $z_j = 5z_j'$, $c^* = 5c'^*$ and $l = l'/5 = i$, we obtain the usual expression for an averaged unit cell slab with dimensions $a, b, c = c'/5$:

$$F(h, k, l) = \sum_j f_j \exp 2\pi i (hx_j + ky_j + lz_j)$$

The Bragg-like diffraction spots were measured on an Enraf-Nonius CAD4 diffractometer (graphite monochromator) at 100 K. Details of the data collection are summarized in Table 1. In order to have sufficient resolution in the X-ray data, especially in the direction perpendicular to the diffuse scattering planes, data were collected to 0.6 \AA ($2\theta \approx 74^\circ$). The Bragg-like diffraction data were indexed on the basis of the reduced, average unit cell slabs, i.e., $l = l'/5$. They display *mmm* Laue symmetry ($R_{\text{int}} = 0.0259$) and systematic absences

Table 1. Crystallographic Data and Structure Refinement

empirical formula	C ₂₀ H _{32.6} N _{0.6} O _{0.4}
formula weight	287.89
cryst syst	orthorhombic (<i>mm</i> 2)
space group	<i>Cmc</i> 2 ₁
<i>a</i> (Å)	15.023(2)
<i>b</i> (Å)	23.198(2)
<i>c</i> (Å)	4.730(1)
α (deg)	89.99(1)
β (deg)	90.00(1)
γ (deg)	90.00(1)
<i>V</i> (Å ³)	1648.4
<i>Z</i>	4
<i>D</i> (calcd) (g cm ⁻³)	1.16
absp coef (mm ⁻¹)	0.135
<i>F</i> (000)	936
cryst size (mm)	0.3 × 0.25 × 0.3
λ (Å)	0.71069
<i>T</i> (K)	100(2)
θ range (deg)	1.61–36.94
index ranges	–17 ≤ <i>h</i> ≤ 16, 0 ≤ <i>k</i> ≤ 27, 0 ≤ <i>l</i> ≤ 8
no. of reflns collected	1674
no. of ind reflns	1003 [<i>R</i> (int) = 0.0259]
abs corr	not done
refinement method	full-matrix least-squares on <i>F</i> ²
data/restraints/param	1003/32/124
weights	$w = (\sigma^2 + g F(hkl) ^4)^{-1}$
GOF on <i>F</i> ²	1.380
final <i>R</i> indices [<i>I</i> > 2 σ (<i>I</i>)]	<i>R</i> ₁ = 0.0429, <i>wR</i> ₂ = 0.0834
(all data)	<i>R</i> ₁ = 0.0900, <i>wR</i> ₂ = 0.0879
absolute struct param	2(10)
extinction coeff	0.0047(11)
largest diff. peak and hole (e Å ⁻³)	0.206 and –0.123

corresponding to the space group *Cmcm* or *Cmc*2₁.¹⁰ The averaged structure was solved by direct methods. In both space groups disordered stacks of superimposed (+)- and (–)-PHTP molecules were found, whose mean planes coincide with each other and are perpendicular to *c*. As far as the PHTP molecules are concerned, the space group of the average structure is thus *Cmcm*. Carbon atoms of the host molecule were refined anisotropically and with population 0.5; hydrogen atoms of the host were added in calculated positions with C–H distances fixed at 1.00 Å.

A difference Fourier synthesis showed high residual electron density in the channels formed by the PHTP molecules. This density was assigned to the atoms of the NPP guest molecule on the basis of the following considerations: Comparison of the cross-section of the channel with the dimensions of NPP requires the long axis of NPP to coincide with the channel axis to within a few degrees. The length of the guest molecule is estimated from standard bond distances and angles¹¹ to be about $c'/2 = 5c/2$. This implies two NPP molecules per *c'* translation or ²/₅ molecules per average slab. In both space groups, the two NPP guest molecules must be mirror symmetric with respect to the *b,c* plane and related by a 2₁ symmetry operation along *c*. This leads to polar chains of NPP molecules interacting via –NO₂⋯HN-hydrogen bonds in any given channel. The chains in different channels may be parallel or antiparallel. If all chains are parallel, the proper space group pertaining to the NPP guest molecules in the average structure is *Cmc*2₁; if the chains are randomly pointing upward or downward, it is *Cmcm* on average. Both possibilities have been tested.

Fractional atomic coordinates *x*_{*j*}, *y*_{*j*}, *z*_{*j*}' for the guest molecule were estimated from standard distances and angles, taking into account the mirror symmetry perpendicular to *a* present in both *Cmc*2₁ and *Cmcm*.

(10) Although no Friedel pairs have been measured, the most probable Laue group is *mmm* because anomalous differences for these C, H, N, O-compounds are exceedingly small. The absolute polarity of the specimen and the possibility of twinning perpendicular to (001) could therefore not be investigated. Note that the monoclinic (*m*) cell given in ref 8 is related to the orthorhombic one used here by the transformation $a_m = (a + b)/2$, $c_m = (a - b)/2$, $b_m = c = c'/5$.

(11) Allen, F. H.; Kennard, O.; Watson, D. G.; Brammer, L.; Orpen, A. G.; Taylor, R. *International Tables of Crystallography*; Kluwer Academic Publishers: Dordrecht, The Netherlands, 1992; Vol. C, pp 685–706.

The coordinates were transformed to $z_j = 5z_j' + \Delta z$ to correspond with the average structure slab. The constant Δz was varied from 0 to 0.5 in steps of 0.05 to test different positions of the guest molecules relative to those of the host molecules. With these starting coordinates least-square refinements were performed in space groups *Cmcm* and *Cmc*2₁ with a set of interatomic distance and planarity restraints derived from the Cambridge Structural Data Base¹² and listed in the Supporting Information. The guest atoms were given individual isotropic displacement parameters. Hydrogen atoms were added in calculated positions with a fixed C–H distance of 1.00 Å. The PHTP atoms were treated as in the preliminary refinement described above. The best agreement factors obtained in the *Cmcm* series of refinements are $wR_2 = 0.0943$, $R_1[|F| > 4\sigma(F)] = 0.0469$, $GOF(F^2) = 1.480$, GOF (including restraints) = 1.464. Those in the *Cmc*2₁ series are consistently lower, $wR_2 = 0.0879$, $R_1[|F| > 4\sigma(F)] = 0.0429$, $GOF(F^2) = 1.380$, GOF (including restraints) = 1.366 (Table 1). These values refer to all 1003 observations unless indicated otherwise. The number of refined parameters is 120 in both series. The values of wR_2 for the two space groups are very close and, according to a Hamilton *R*-factor ratio test,¹³ *Cmcm* cannot be rejected at the 0.05 significance level. This lack of discrimination persists independently of the factor *g* used to downweigh the strong reflections (9.43 vs 8.79% for *g* = 0.03; 6.04 vs 6.08% for *g* = 0; 11.12 vs 11.45% for *g* = 0.06). At this point two questions arise: (1) Why are the wR_2 -values so similar for the two space groups? (2) Is wR_2 the most suitable indicator to distinguish between the polar space group *Cmc*2₁ and the centrosymmetric variant *Cmcm*?

Analyzing the coordinates of the guest molecules, it is found that the O₂NC₆H₄N(CH₂)₂ fragment is pseudo mirror symmetric with respect to the mirror plane perpendicular to *c* and pertaining to the disordered PHTP molecules ($z = 1/4$, Figure 3). Thus, a CH₂NHCH₂ fragment is the only part of the otherwise centrosymmetric structure which allows us to distinguish between *Cmc*2₁ and *Cmcm*. The total number of atoms in the average unit cell slab is C₈₀H_{130.4}N_{2.4}O_{1.6}, representing a scattering power of 640 electrons; the corresponding number for the distinguishing CH₂NHCH₂ fragment is 19.2 electrons, a mere 3% of the total scattering power. Global disagreement factors such as wR_2 , which are obtained from all observations, measure the overall disagreement between the data and the refinement model. They are dominated by the large deviations $w\Delta(F^2)$ arising mainly from the strong reflections, whereas a distinction between a centrosymmetric and a non-centrosymmetric space group is expected to be seen in the weak reflections.¹⁴ Thus, a more powerful discriminator is desirable, related more directly to the features distinguishing the two structures.¹⁵ In the case at hand, a population parameter *p* has been refined which measures the percentage of guest molecules pointing along one direction of the channels; (100 – *p*) represents the percentage of molecules pointing in the opposite direction. Such a parameter is specific for the electron density within the channels and does not depend directly on the host molecules. The results of these refinements are found to be independent of the weighting scheme: *p* is 101(5), 95(4), and 97(4)% for weight modifications *g* of 0.00, 0.03, and 0.06, respectively. To test the influence of the weakest, least reliable reflections on these results, an analogous set of refinements was performed on 604 strong reflections with $F^2 > 2\sigma(F^2)$ and weight modifications as above. Resulting values of wR_2 and *p* are 6.01, 8.91, and 11.27% and 100.5(6.5), 93(6), and 95(5) %, respectively. For a random up and down orientation of guest chains in different channels, the expected value of *p* would have been 50%. It is thus safe to conclude that the space group of the average structure slab is *Cmc*2₁ and that the hydrogen bonded chains of NPP molecules show a parallel rather than an antiparallel alignment in the disordered crystal structure.^{16,17}

(12) Allen, F. H.; Davies, J. E.; Galloy, J. J.; Johnson, O.; Kennard, O.; Macrae, C. F.; Mitchell, E. M.; Mitchell, G. F.; Smith, J. M.; Watson, D. G. *J. Chem. Inf. Comput. Sci.* **1991**, *31*, 187.

(13) Hamilton, W. C. *Statistics in Physical Science*; Ronald Press Company: New York, 1964.

(14) (a) Dunitz, J. D. *X-Ray Analysis and the Structure of Organic Molecules*; Cornell University Press: Ithaca, NY, 1979. (b) Marsh, R. E. *Acta Crystallogr.* **1995**, *B51*, 897–907. (c) Watkin, D. *Acta Crystallogr.* **1994**, *A50*, 411–437.

(15) Schwarzenbach, D.; Abrahams, S. C.; Flack, H. D.; Prince, E.; Wilson, A. J. C. *Acta Crystallogr.* **1995**, *A51*, 565–569.

(16) An analogous refinement for the PHTP molecules gives 50.02(6)%.

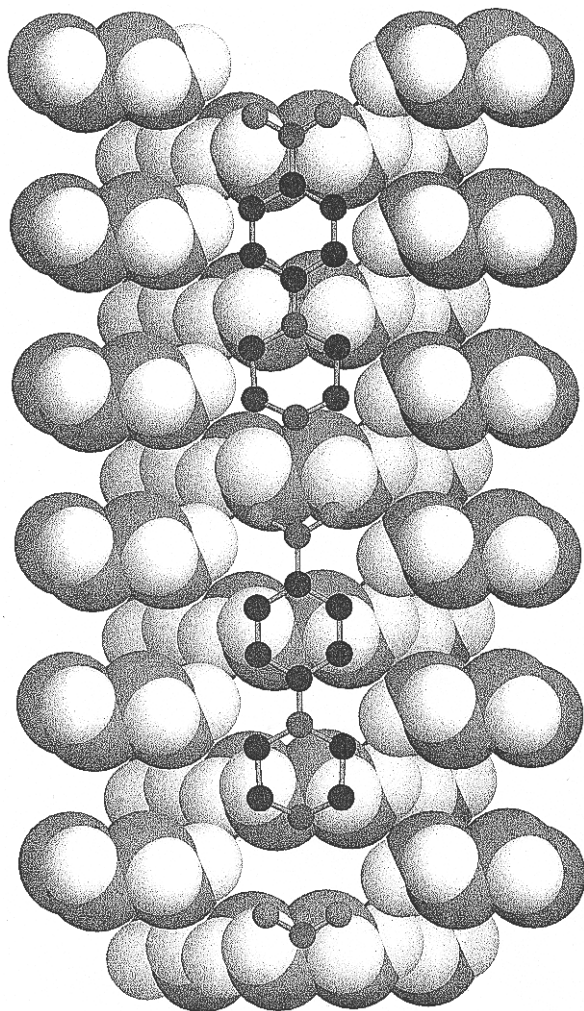


Figure 3. Two NPP guest molecules embedded in a channel of PHTP host molecules; projection along b . (Host carbon atoms dark grey, van der Waals radii; equatorial hydrogen atoms grey, van der Waals radii reduced to 70%; axial hydrogen atoms not shown. Guest atoms, van der Waals radii, reduced to 20%, no hydrogen atoms shown.) Plotted with the program ATOMS, shape software.

Results of the $Cmc2_1$ refinement with p fixed to 100% and a weight modification factor of 0.03 are given in the Supporting Information (atomic coordinates, restraints, bond distances and angles, H-coordinates, and anisotropic displacement parameters). The implications of these results are discussed in the Results and Discussion section. All calculations were performed with the programs SHELXL93¹⁸ and XS.¹⁹

In view of the unusual observed diffraction pattern, it seems worthwhile to mention a number of crystallographic details which allow judgement of the quality of the structure analysis as a whole. The number of reflections with $|F_{\text{obsd}} - F_{\text{calcd}}| > 3\sigma(F_{\text{obsd}})$ is 9. Assuming a Gaussian distribution of $|F_{\text{obsd}} - F_{\text{calcd}}|/\sigma(F_{\text{obsd}})$, the expected number is only slightly smaller at ~ 3 . The maximum deviation is $4.91\sigma(F_{\text{obsd}})$. The values of the bond distances and their estimated standard deviations used as restraints are listed in the Supporting Information; they have been taken from ref 11 and represent the results of 1116 individual structure determinations. The average mean square deviations $\langle \Delta^2/\sigma^2 \rangle$ from the target values are 0.89 for the distance restraints and 0.15 for the planarity restraints imposed on the N-C₆H₄-NO₂ fragment, i.e., the restraints are obeyed better than expected on statistical grounds ($\langle \Delta^2/\sigma^2 \rangle = 1$). Since in the average structure slab

(17) The possibility of monoclinic twinning has also been explored. Refinements in space groups $C1c1$, or $C112_1$ with (100) as twin plane lead to wR_2 of ~ 25 –30%.

(18) Sheldrick, G. M. SHELXL93, program for the refinement of crystal structures; University of Göttingen, Germany, 1993.

(19) SHELXTL PC, SIEMENS Analytical, X-ray Instruments, Inc., Madison, WI, 1990.

the atoms O1, C2, C3, C5, C6 and N1, C1, C4, N2, N3, respectively, are partially superimposed (pseudo mirror symmetry, see above) it was necessary to restrain their isotropic displacement parameters to be the same to within $\sigma = 0.005 \text{ \AA}^2$; $\langle \Delta^2/\sigma^2 \rangle$ is 1.03, i.e., equal to the statistical expectation value of this quantity; ranges of refined U values are 0.014–0.025(3) \AA^2 for C and N, comparable to the range of U_{eq} for the PHTP carbon atoms 0.021–0.034(2) \AA^2 ; $U(\text{O1})$ is somewhat larger at 0.040(3) \AA^2 , indicating torsional vibration or disorder of the NO₂ groups. The final difference Fourier synthesis shows 14 peaks in the range of 0.21–0.10(3) $e \text{ \AA}^{-3}$. The first 10 of them are located on centers of PHTP C–C bonds and indicate residual bonding electron density. This shows that there is essentially no electron density which cannot be accounted for in terms of our structural model.

The weak reflections superimposed on the diffuse layers at $h \pm 0.62(1)$, k , $5i \pm 1$ ($h+k$ even) and $h,k,5i \pm 2$ ($h+k$ odd) contain information on the probability that NPP molecules m (or $m + 1/2$) and n (or $n + 1/2$) translations apart along a and b , differ in their z' coordinates by $q/5 = 0, 0.2, 0.4, 0.6$, or 0.8 fractional coordinate units. If the weak reflections were absent, all probabilities $P(q)$ would be equal to 0.2. Their presence indicates a residual correlation of q between different channels. These reflections have not been measured so far, because they are very weak and their reflection profiles show fine structure which is difficult to interpret. Similarly, the percentage distribution of intensity between Bragg-like peaks, weak reflections, and diffuse features have not yet been measured, thus precluding any reliable conclusion about the function $P[q(m,n)]$.

Results and Discussion

The Crystal Structure. It was shown in the previous section (and can be seen from Figure 2) that crystals of $[(\pm)\text{-PHTP}]_5\text{-[NNPP]}$ exhibit several kinds of disorder and that only an *averaged crystal structure* can be determined easily. What can be said about the *real structure* of this polar material? First, we discuss the crystal architecture of the PHTP host molecules. Second, we analyze the arrangement of the NPP guest molecules relative to the host lattice. Third, we address the nature of the interaction between host and guest. Finally, the crystal structure is discussed in relation to its physical properties and in relation to qualitative morphological observations made when the tailor made, less-polar additive TP is present during crystallization.

The host lattice is built from stacks of PHTP molecules extending along c' . The stacks occupy the corners of a honeycomb motif and surround a channel whose walls are decorated with equatorial CH₂ hydrogen atoms of PHTP (Figures 1 and 3). This arrangement is similar to that found in many other host–guest cocrystal phases of PHTP²⁰ except that here the van der Waals diameter of the channels is wider along a (5.9 \AA) and narrower along b (3.9 \AA), commensurate with the intermediate and small van der Waals diameters of NPP. There are five PHTP molecules per c' translation unit but the average structure shows statistically disordered (+)-PHTP and (–)-PHTP molecules and thus gives no information on the spatial distribution of enantiomers. An ordered alternating arrangement of (+)- and (–) molecules within one stack is impossible because this would require a translation period of $2c'$, i.e., 10 PHTP molecules. Furthermore, such an arrangement would require that 9 axial hydrogen atoms on one PHTP eclipse 9 axial hydrogen atoms of the neighboring PHTP at a rather short distance of $\sim 2.1 \text{ \AA}$.²¹ For stacks of homochiral molecules, the two groups of 9 axial hydrogen atoms show a staggered arrangement with more reasonable H \cdots H distances of $\sim 2.5 \text{ \AA}$. In addition, the stacking distance in the enantiomerically pure $[(\pm)\text{-PHTP}]_5\text{[NPP]}$ system, where the H \cdots H arrangement must

(20) Farina, M. In *Inclusion Compounds 2*; Atwood, J. L., Davis, J. E. D., MacNicol, D. D., Ed.; Academic Press: London, 1984.

(21) This value represents the *internuclear* H \cdots H distance assuming a C–H *internuclear* bond distance of 1.09 \AA , rather than the systematically shorter distance of 1.00 \AA between C and H electron density maxima.

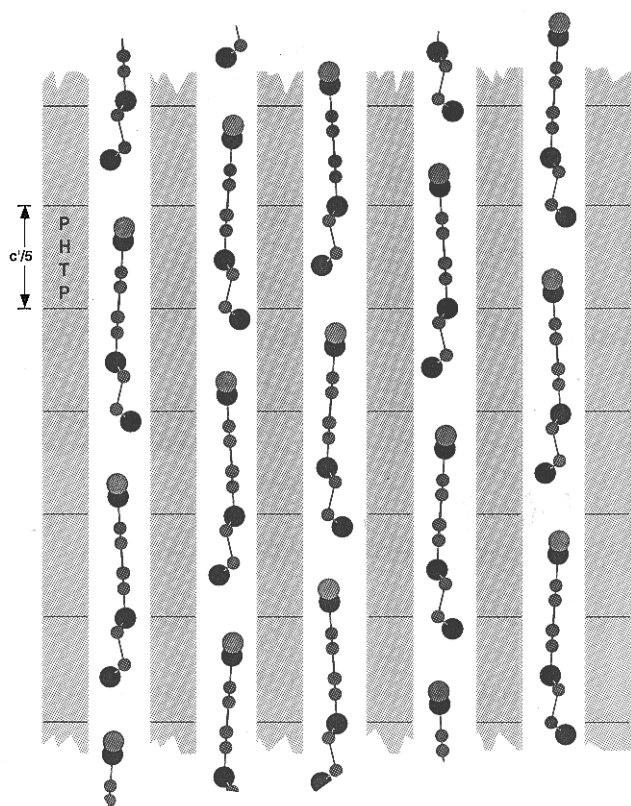


Figure 4. Schematic drawing showing the register along c' of NPP molecules relative to PHTP molecules. NPP positions differ by integer multiples of $c'/5$; the probabilities of the positions as a function of the number of intervening channels is under investigation.

be staggered, is 4.76 Å (at 295 K), very close to the value of 4.73 Å (at 100 K) in the racemic compound. Both observations indicate that an individual stack is built from *homochiral* PHTP molecules and that (+)-PHTP and (–)-PHTP stacks are randomly distributed throughout the crystal. This substantiates earlier observation of Farina which was based on much less detailed experimental evidence.²⁰ Neighboring PHTP stacks are displaced relative to each other by $c/2 = 2.37$ Å. Their packing is dominated by the 12 equatorial hydrogen atoms per PHTP molecule. These atoms are situated almost in the mean PHTP plane, to within ± 0.15 Å.²² This leads to approximate mirror planes perpendicular to the PHTP stacks and implies that the interaction energy between homochiral stacks differs little from that between enantiomeric ones. Thus, the disordered arrangement of (+)- and (–)-stacks is not too surprising.

The NPP guest molecules occupy well-defined positions in the channels of the host lattice. The centers of the phenyl rings coincide to within 0.05 Å with the mean plane of a neighboring PHTP molecule. The chromophoric fragment $\text{NC}_6\text{H}_4\text{NO}_2$ is inclined by only 4° relative to the channel axis. Consecutive NPP molecules interact via $\text{-NO}_2 \cdots \text{HN-}$ hydrogen bonds with $\text{O} \cdots \text{N}$ and $\text{O} \cdots \text{H}$ distances of 3.1 and ~ 2.2 Å, respectively (Figure 3). The NPP molecules are related by 2-fold screw operations and form infinite polar chains. Chains in adjacent channels are displaced relative to each other along the c axis. The magnitude of the displacement is an integer multiple of $c'/5$ (Figure 4). The relative probabilities of each of these displacements have not yet been determined but the presence of weak reflections on the diffuse scattering planes permits us to conclude that these probabilities are generally different from $1/5$. It cannot entirely be excluded that some kind of short-

range order of the PHTP stacks also contributes intensity to these reflections.

Our diffraction analysis demonstrates that the chains in different channels of $[\text{PHTP}]_5[\text{NPP}]$ show *parallel alignment* with a probability of $\geq 95\%$. The overall crystal structure is thus *polar*, in agreement with the observed SHG, the EO, and the pyroelectric effects. But which are the factors leading to macroscopic polarity?

The guest molecule is highly polar with a hydrogen-bond donor (-NH) at one end and an acceptor (-NO_2) at the other end; furthermore, the $\text{NC}_6\text{H}_4\text{NO}_2$ chromophore is polarizable with an electron-donating aniline group at one end and an accepting nitro group at the other. This explains the polar arrangement of NPP molecules in a single channel mediated by $\text{NO}_2 \cdots \text{HN}$ hydrogen bonds. However, it is relatively difficult to explain the long-range polar ordering of neighboring channels in terms of guest–guest interactions. Neighboring channels are separated by ~ 15 Å (along a) or ~ 14 Å (along $(a + b)/2$); thus, any direct electrostatic interaction energy between channels is quite small compared to the temperature of crystallization (~ 100 J/mol per 0.1 electrostatic charge vs $RT = 2.5\text{--}3.1$ kJ/mol).

It is similarly difficult to explain the long-range polar ordering in terms of host–guest interactions. Because the PHTP stacks show approximate mirror symmetry perpendicular to c' , they do not impose a significant polarity on the channel walls, even if they were formed by six homochiral stacks. Alternatively, one might argue in terms of lateral displacements (in the a, b plane) of PHTP host molecules, either in the bulk or on growing prismatic crystal faces. The argument implies that an open half-channel on the surface of a growing prismatic face shows an imprint of the NPP molecule in the channel below the crystal surface, corresponding to a possible steric transmission of packing information. Of course, the crystal structure says little, if anything, about the finer details of surface structure. We can only test the bulk structure for remaining indications of such an imprint. A sideways modulation of the five PHTP molecules, producing a better fit to the two NPP molecules per c' translation unit, would have to reveal itself in the atomic displacement parameters U_{11} , U_{22} , and U_{12} of the PHTP molecule in the average structure slab. The values U_{11} and U_{22} vary from 0.021 to 0.034 Å². If we assume, conservatively, that about one-half of these values is due to thermal motion and the other half to the postulated static modulation, then the static displacements would be ~ 0.1 Å. In comparison with the shortest $\text{H} \cdots \text{H}$ interaction of ~ 2.40 Å between PHTP and NPP, this again is a small effect. Arguing in terms of a tilt of the PHTP molecules relative to the channel axis is similarly inconclusive. Seen in this light, the parallel arrangement of the polar chains is a remarkable fact.

Results on Measured Physical Properties and Crystal Growth. Whatever the mechanism responsible for the macroscopic polarity turns out to be, it is intimately connected to the *crystal growth process*. Once the guest molecules are included in the channel architecture, the host lattice prevents reversal of molecular dipoles. The growth mechanism is hence entirely responsible for the final state of orientation of the molecular dipoles.

A monodomain of crystalline $[\text{PHTP}]_5[\text{NPP}]$ with average $mm2$ symmetry could display a number of growth properties reflecting polar symmetry. These include: (i) lack of centrosymmetrically related faces due to different growth velocities $R(hkl)$ and $R(\bar{h}\bar{k}\bar{l})$; (ii) different etching rates and topographies of etched faces with (hkl) and $(h\bar{k}\bar{l})$ indices; etch pits on prismatic

(22) The corresponding deviations of the carbon atom is ± 0.24 Å; that of the axial hydrogen atoms is ± 1.25 Å.

faces with polar symmetry;²³ and (iii) different molecular recognition of the donor and acceptor decorated end faces of the needle by appropriately substituted species in solution, e.g., TP.

Our growth experiments performed on the [PHTP]₅[NPP] system allow the following comments on (i) and (ii):

(i) [(±)-PHTP]₅[NPP] crystals grown from 2-butanone show a needle-like habit with flat prismatic (120), ($\bar{1}20$), (210), ($\bar{2}10$), (140) and ($\bar{1}40$) faces. The capping faces are irregular (rough)²⁴ and do not permit any conclusions concerning polar symmetry. This might be a result of the molecular roughness caused by the 2-dimensional disorder of NPP molecules along *c'*. The prismatic faces show macroscopic monoclinic symmetry, whereas the unit cell dimensions and the agreement factor of 0.026 between equivalent diffraction intensities (see Table 1) indicates an average orthorhombic symmetry at the microscopic level. The reasons for this difference are not understood at present.

Observation of the spontaneous nucleation and subsequent growth of needle-shaped crystals with a video camera does not show different growth velocities along the +*c* and the -*c* directions. Similar growth experiments on a number of pure NLO compounds containing amino and nitro groups as hydrogen-bond donors and acceptors revealed a pronounced asymmetry in corresponding velocities.²⁵ Although the capping surfaces of [PHTP]₅[NPP] crystals exhibit a density of donor and acceptor groups which is ~10 times lower than that of pure NLO crystals, one would nevertheless expect a measurable effect on the difference of growth velocities. A possible explanation for the lack of an observable difference could be the formation of needles *twinned* relative to the (001) plane. The observed reversal of the pyroelectric polarity along *c* is compatible with such a twinning. The sign of the effect indicates that the caps are decorated with NO₂ groups.

(ii) Etching of polished (001) faces (HCl, 0.1–1 M) produced hexagonally shaped etch pits, but no detectable difference in the topography of (001) and (00 $\bar{1}$) faces. Similar etching experiments on prismatic (*hk0*) faces did not reveal etch pits typical of polar symmetry. Again, the expected asymmetric etch features have been observed on corresponding crystal faces of the pure NLO substances mentioned above.²⁶ Their absence is compatible with the average mirror symmetry of the host lattice perpendicular to *c*.

Summing up the experimental observations on crystal growth and physical properties, we can say the following: (1) Different methods of crystallization on different surfaces consistently produce polar material. This suggests that the observed polarity is not due to accidental effects of the growth medium, but is an intrinsic attribute of [PHTP]₅[NPP] crystals or of the nucleation and growth processes. (2) The X-ray diffraction study indicates polar domains with a length of at least 100 Å (corresponding to >10 NPP molecules). (3) SHG, observed with a fundamental wavelength of about 1 μm, indicates polarity. (4) The EO and pyroelectric measurements also show predominance of domains of one polarity within the illuminated or heated crystal volume. (5) The reversal of the pyroelectric effect along *c* and the lack of polar growth properties indicate twinning relative to the (001) plane.

Discussion of Physical Properties and Crystal Growth. These observations can be accounted for qualitatively by a

(23) Heimann, R. B. *Auflösung von Kristallen*; Springer: Wien, 1975.

(24) Optical microscopy (interference contrast) and atomic force microscopy showed only rough faces, i.e., faces with a high density of macrosteps.

(25) Hulliger, J. ETH Zürich 1992, unpublished work. Hulliger, J.; Bržina, B.; Ehrensperger, M. *J. Cryst. Growth* **1990**, *106*, 605–610.

(26) Bržina, B.; Hulliger, J. *Cryst. Res. Technol.* **1991**, *26*, 155–160.

simple model²⁷ for the growth along *c*. Given a crystal nucleus, the rough end faces will grow by adding PHTP molecules to the hydrocarbon stacks and NPP molecules to the channels. During this process the PHTP stacks must chose between PHTP molecules of opposite chirality. The steric fit of the PHTP molecule at the end of a stack to a homochiral PHTP molecule from solution shows better shape complementarity than to a heterochiral molecule, hence the host stacks tend to be homochiral. For growth within the channels, two situations may occur: (1) The last molecule in the channel exposes a NO₂ group to the surface. The preferred mode of attachment for the next NPP molecules will be through hydrogen bonding to the HN group. The reverse attachment -NO₂ on O₂N-, is very much less probable; i.e., a change of decoration of the surface from O₂N- to HN groups is very rare. (2) The last molecule in the channel exposes its HN group to the surface. The preferred mode of attachment for the next NPP molecule will be through hydrogen bonding to the NO₂ group. The reverse attachment, -NH on HN-, is less probable, but not as bad as -NO₂ on O₂N-, because the amine hydrogen atom of one piperazine ring can go axial to allow the formation of an H_{ax}N···H_{eq}N hydrogen bond. Thus, the process whereby a cap decorated with HN groups changes to NO₂ decoration is more likely than the reverse process. The *difference in the probabilities* of forming -NO₂···O₂N- and -NH···HN- contacts thus leads to preferred exposure of NO₂ groups on the capping faces during growth. This conclusion applies even if initially a capping face of a seed crystal is decorated primarily by HN groups. Ultimately, the growing crystal will expose mostly NO₂ groups on *both* caps, irrespective of the initial decoration of the two ends of the nucleus. This implies that macroscopically the crystal is a twin of two polar domains with their polar axes antiparallel in agreement with the space resolved measurements of the pyroelectric effect. For such a twin, the growth rates along ±*c* will be the same as observed.

The qualitative description of the growth mechanism given above can be expressed algebraically in terms of a *Markov* process:²⁸ Given *N* channels on a cap, *n*^o_{NO₂} channels initially expose an NO₂ group and *n*^o_{NH} channels an HN group. Growth is controlled by the probabilities *p*(NO₂···HN), *p*(NO₂···O₂N), *p*(NH···O₂N), and *p*(HN···HN) for forming -NO₂···HN-, -NO₂···O₂N-, -NH···O₂N-, and -HN···HN- contacts, respectively. After adding *r* NPP molecules to each channel, *n*^r_{NO₂} channels expose an NO₂ group and *n*^r_{NH} channels an NH group. The final situation is related to the initial on by

$$\begin{bmatrix} n_{\text{NO}_2}^r \\ n_{\text{NH}}^r \end{bmatrix} = \begin{bmatrix} p(\text{NO}_2 \cdots \text{HN}) & p(\text{HN} \cdots \text{HN}) \\ p(\text{NO}_2 \cdots \text{O}_2\text{N}) & p(\text{HN} \cdots \text{O}_2\text{N}) \end{bmatrix}^r \cdot \begin{bmatrix} n_{\text{NO}_2}^o \\ n_{\text{NH}}^o \end{bmatrix}$$

Note that *p*(NO₂···O₂N) + *p*(NO₂···HN) = *p*(HN···HN) + *p*(NH···O₂N) = 1. If the number of added molecules is sufficiently large, the above relation simplifies to

$$\begin{bmatrix} n_{\text{NO}_2}^r \\ n_{\text{NH}}^r \end{bmatrix} = \begin{bmatrix} \bar{p}(\text{NO}_2) & \bar{p}(\text{NO}_2) \\ \bar{p}(\text{NH}) & \bar{p}(\text{NH}) \end{bmatrix} \cdot \begin{bmatrix} n_{\text{NO}_2}^o \\ n_{\text{NH}}^o \end{bmatrix} = \begin{bmatrix} \bar{p}(\text{NO}_2) \cdot N \\ \bar{p}(\text{NH}) \cdot N \end{bmatrix}$$

(27) Hulliger, J.; Rogin, P.; Quintel, A.; Rechsteiner, P.; König, O.; Wübbenhorst, M. *Adv. Mater.* **1997**, *9*, 677–680.

(28) After this work had been submitted, we became aware of a recent publication: Harris, K. D. M.; Jupp, P. E. *Proc. R. Soc. London A*, **1997**, *453*, 333. The model of sequential crystal growth described by these authors is essentially the same as the one developed in this work and similar to the arguments in ref 27. For mathematical details, see: Zachmann, H. G. *Mathematik für Chemiker*, 5th ed; Verlag Chemie: Weinheim, 1994. Gardiner, C. W. *Handbook of Stochastic Methods*, 2nd ed.; Springer: Berlin, 1997.

The selectivities $\bar{p}(\text{NO}_2)$ and $\bar{p}(\text{NH})$ are defined as

$$\bar{p}(\text{NO}_2) = p(\text{HN}\cdots\text{HN})/[p(\text{NO}_2\cdots\text{O}_2\text{N}) + p(\text{HN}\cdots\text{HN})]$$

$$\bar{p}(\text{NH}) = p(\text{NO}_2\cdots\text{O}_2\text{N})/[p(\text{NO}_2\cdots\text{O}_2\text{N}) + p(\text{HN}\cdots\text{HN})]$$

and are seen to depend only on the error rates. It is likely that $p(\text{HN}\cdots\text{HN}) > p(\text{NO}_2\cdots\text{O}_2\text{N})$ and thus $n'_{\text{NO}_2} > n'_{\text{NH}}$, irrespective of $n^{\circ}_{\text{NO}_2}$ and n°_{NH} . This implies, that the capping faces on both sides of a crystal preferentially expose NO_2 groups in agreement with the observed sign of the pyroelectric effect and its reversal along c .

The probabilities in this model are proportional to the attachment energies according to

$$p(\text{NO}_2\cdots\text{HN}) \propto \exp[-\Delta G(\text{NO}_2\cdots\text{HN})/RT]$$

$$p(\text{NO}_2\cdots\text{O}_2\text{N}) \propto \exp[-\Delta G(\text{NO}_2\cdots\text{O}_2\text{N})/RT]$$

$$p(\text{HN}\cdots\text{HN}) \propto \exp[-\Delta G(\text{HN}\cdots\text{HN})/RT]$$

$$p(\text{NH}\cdots\text{O}_2\text{N}) \propto \exp[-\Delta G(\text{NH}\cdots\text{O}_2\text{N})/RT]$$

If it is assumed that $\Delta G(\text{NO}_2\cdots\text{HN}) \approx \Delta G(\text{NH}\cdots\text{O}_2\text{N})$, it follows that

$$p(\text{HN}\cdots\text{HN})/p(\text{NO}_2\cdots\text{O}_2\text{N}) = \exp[-\{\Delta G(\text{HN}\cdots\text{HN}) - \Delta G(\text{NO}_2\cdots\text{O}_2\text{N})\}/RT]$$

The crystal structure determination indicates that in a homopolar domain of the crystal more than 95% of the NPP molecules point in one direction and only less than 5% in the other. From this result, we obtain

$$\bar{p}(\text{NO}_2)/\bar{p}(\text{NH}) = p(\text{HN}\cdots\text{HN})/p(\text{NO}_2\cdots\text{O}_2\text{N}) > 20$$

corresponding to an energy difference $\Delta G(\text{NO}_2\cdots\text{O}_2\text{N}) - \Delta G(\text{HN}\cdots\text{HN})$ of 8 kJ/mol or more ($T \approx 300$ K).

A lower limit for the other energy differences can be obtained, if we assume, rather conservatively, $p(\text{NH}\cdots\text{O}_2\text{N})/p(\text{HN}\cdots\text{HN}) \approx 1$. Then, $\Delta G(\text{HN}\cdots\text{HN}) - \Delta G(\text{NO}_2\cdots\text{HN}) \approx 0$ and $\Delta G(\text{NO}_2\cdots\text{O}_2\text{N}) - \Delta G(\text{NO}_2\cdots\text{HN}) \geq 8$ kJ/mol. A more realistic estimate is $p(\text{NH}\cdots\text{O}_2\text{N})/p(\text{HN}\cdots\text{HN}) \geq 10$; the energy differences are then >6 and >14 kJ/mol, respectively.

The probability distribution of polar domains with m NPP molecules in a single channel, i.e., of sequences such as $(\text{O}_2\text{N-R-NH})\cdots(\text{HN-R-NO}_2)_m\cdots(\text{O}_2\text{N-R-NH})$ ($R =$ bridging fragment of NPP), is $p(m) = \bar{p}(\text{NH}) \cdot p(\text{HN}\cdots\text{HN}) \cdot p(\text{NO}_2\cdots\text{HN})^{m-1} \cdot p(\text{NO}_2\cdots\text{O}_2\text{N})$. The most probable length is $-\{\ln p(\text{NO}_2\cdots\text{HN})\}^{-1}$; the mean length is twice as long because the distribution is strongly skewed, and the root-mean-square deviation from the mean is $-3^{1/2}[\ln p(\text{NO}_2\cdots\text{HN})]^{-1}$. For the estimate termed realistic above, $p(\text{NO}_2\cdots\text{HN})$ is ≥ 0.995 and the mean length is $m \geq 400$, corresponding to ≥ 5000 Å. Similarly, the most probable length for sequences $(\text{HN-R-NO}_2)\cdots(\text{O}_2\text{N-R-NH})_m\cdots(\text{HN-R-NO}_2)$ with reversed polarity is obtained from $p(\text{NH}\cdots\text{O}_2\text{N}) \approx 0.1$ to be ~ 20 . Thus, both halves of the crystal are characterized by chains >400 NPP molecules long, whose NO_2 groups are pointing to the growing caps, interspaced with much shorter reversed sequences; i.e., both halves of the crystal are macroscopically polar.²⁹ This explains the observed SHG, pyroelectric, and EO effects.

Habit Modification and Alteration of Polar Properties in the Presence of a Tailor-made Additive. As discussed in the previous section, the rough capping faces of growing NPP crystals are decorated primarily with NO_2 groups. TP (1-(p -

tolyl)piperazine) can thus act as a tailor-made additive as described by Lahav, Leiserowitz, and their collaborators.³⁰

TP adds to the growing crystal via its HN group with a probability similar to that of NPP. Further growth always forces an energetically unfavorable $-\text{CH}_3\cdots\text{O}_2\text{N}-$ or an even less favorable $-\text{CH}_3\cdots\text{HN}-$ contact. Adsorption of TP molecule at a O_2N surface site thus retards the crystal growth velocity along c . Growth of the prismatic faces is affected differently. It involves filling of the half-open PHTP host channels by NPP or TP and completion of the channels by PHTP host molecules. Both of these processes depend predominantly on weak host-guest or host-additive interactions which would seem to differ relatively little compared to the various guest-guest and guest-additive interactions controlling growth along c . The observed habit modification from a prismatic to a plate-like shape induced by TP can thus be explained by a retardation of growth along c relative to growth of the prismatic faces.

Coinclusion of as little as 7 mol % PT into $[\text{PHTP}]_5-[(\text{NPP})_{1-x}(\text{TP})_x]$ reduces the SHG response below the limit of visual detection. This is consistent with the growth mechanism described for the pure compound. After incorporation of a TP molecule into the channel, the probability for continuing the same polarity is $p(\text{CH}_3\cdots\text{HN})$, that for reversing the polarity is $p(\text{CH}_3\cdots\text{O}_2\text{N})$. We assume, as a first approximation, (1) that these probabilities are nearly equal, i.e., 0.5, and (2) that TP is effectively incorporated into the crystal only if an NPP molecule exposes an NO_2 group. The corresponding Markov matrix becomes

$$\begin{bmatrix} p(\text{NO}_2\cdots\text{HN}) \cdot q/N & p(\text{HN}\cdots\text{HN}) & p(\text{CH}_3\cdots\text{HN}) \\ p(\text{NO}_2\cdots\text{O}_2\text{N}) \cdot q/N & p(\text{NH}\cdots\text{O}_2\text{N}) & p(\text{CH}_3\cdots\text{O}_2\text{N}) \\ p(\text{NO}_2\cdots\text{HN}) \cdot (1-q)/N & 0 & 0 \end{bmatrix}$$

The quantity q describes the competition of NPP and TP for an exposed NO_2 group and depends on the relative concentrations of NPP and TP in the nutrient phase (N is a normalization factor). For a large number r of growth steps, the limiting Markov probabilities become

$$\bar{p}(\text{NO}_2, q), \bar{p}(\text{NH}, q), \bar{p}(\text{CH}_3, q)$$

With increasing competition $(1-q)$ of TP, the ratio of NPP molecules with antiparallel orientation quickly approaches 1, whereas the amount of included TP remains small: As an example we have chosen $q = 0.85$, which reproduces the observed incorporation probability of TP, $\bar{p}(\text{CH}_3, 0.85) = 0.07$. With this choice $\bar{p}(\text{NO}_2, 0.85)$ becomes 0.49 and $\bar{p}(\text{NH}, 0.85)$ is 0.43, to be compared with values of 0.95 and 0.05 in the absence of TP. Thus, incorporation of only a small amount of TP almost balances the two orientations of NPP. Furthermore, the chains in either orientation are now of similar length and much shorter, 10–20 molecules on average. Such a structure is not expected to show SHG or other macroscopic polar properties, in agreement with experimental observation.

In conclusion, the model which explains the observed polar properties of $[\text{PHTP}]_5[\text{NPP}]$ also explains their disappearance in $[\text{PHTP}]_5[(\text{NPP})_{1-x}(\text{TP})_x]$.³¹

(29) Here, we disagree with Harris and Jupp (ref 28, p 351) who argue that their model "will not lead to large-scale asymmetry when many tunnels are present, provided that ... guest molecules enter the tunnels from the left and the right with equal probability". It is true that under these conditions the crystal as a whole is built of two domains whose polarities are related by a plane of symmetry, but each domain individually shows "large-scale asymmetry", as can be seen in both the experiments and the Markov model. In their latest paper, Harris and Jupp (Harris, K. D. M.; Jupp, P. E. *Chem. Phys. Lett.* **1997**, *274*, 525) reach a similar conclusion.

(30) For a review, see: Weissbuch, I.; Popovitz, R.; Lahav M.; Leiserowitz, L. *Acta Crystallogr.* **1995**, *B51*, 115–148.

Conclusions

This work reports, for the first time, a detailed and accurate structure analysis of a PHTP host–guest compound. The structure determination was successful, in spite of the presence of extensive diffuse and satellite scattering, through a qualitative and quantitative analysis of the X-ray diffraction data combined with stereochemical reasoning. The technical feasibility of this analysis is of some interest, because supramolecular crystal synthesis will undoubtedly produce many more examples of materials with interesting properties and severe crystallographic disorder. Quantitative investigations of the diffuse and satellite scattering are in progress.

The diffraction analysis has shown that the polar NPP guest molecules form parallel, $-\text{NO}_2\cdots\text{HN}-$ hydrogen-bonded chains embedded in apolar PHTP channels. The domains of parallel NPP molecules show meso- to macroscopic dimensions. Independent evidence for a polar structure comes from second harmonic generation, electro-optical experiments and a pyroelectric effect. This structure, together with other $[\text{PHTP}]_n[\text{polar guest}]$ systems we have investigated,^{4,8} demonstrates the adaptability of the supramolecular architecture of the PHTP host to the shape of the guest molecules.

This and previous work have shown that cocrystallization of polar molecules PHTP, thiourea, and other channel-forming

(31) Calculations with $q = 0.9, 0.8,$ and 0.7 lead to probabilities $\bar{p}(\text{CH}_3, q)$, $\bar{p}(\text{NO}_2, q)$, and $\bar{p}(\text{HN}, q)$ of (0.06, 0.61, 0.33), (0.09, 0.45, 0.46), and (0.11, 0.35, 0.54), respectively. This indicates that for suitably chosen systems the sign of the polarity can be reversed and thus controlled by an appropriate additive. Models with more complex 4×4 Markov matrices lead to comparable results.

compounds³ with polar molecules produces an unexpectedly high incidence of phases with macroscopic polar properties. This phenomenon can be understood in terms of a growth mechanism analogous to the one described here. For guest molecules with donor (D) and acceptor groups (A) at opposite ends, the relative probabilities of forming $-\text{A}\cdots\text{A}-$ and $-\text{D}\cdots\text{D}-$ contacts will determine the polarity of growing cap faces, and the relative probabilities of forming $-\text{D}\cdots\text{A}-$ vs $-\text{D}\cdots\text{D}-$ or $-\text{A}\cdots\text{A}-$ contacts will determine the average length of polar domains. An extension of this mechanism also accounts for the suppression of polar properties due to coinclusion of a small amount of a tailor-made additive molecule. The mechanism proposed here, together with the tunability of host–guest and guest–guest interactions, provides some of the tools necessary to engineer the crystal structures and physical properties of PHTP and related channel-type inclusion compounds.

Acknowledgment. We thank Prof. P. Sozzani, Department of Material Science, University of Milan, for a sample of enantiomerically pure (–)-PHTP and A. Saxer, University of Berne, and Dr. G. Claude, University of Neuchâtel, for the separation of racemic PHTP. We acknowledge financial support from the Swiss National Science Foundation (project no. 20-43'116'95, NFP 36 no. 4036-043932).

Supporting Information Available: Table of atomic coordinates, bond lengths and angles, anisotropic displacement parameters, hydrogen coordinates, restraints used in the refinement, F_o , F_c and $\sigma(F_o)$ (11 pages). See any current masthead page for ordering and Internet access instructions.

JA971945S